

# Mineralogy of Size Fractions in Sancheong Kaolin and Its Origin

산청고령토 입도분리시료들의 광물조성 변화와 그 원인

Gi Young Jeong(정기영) · Soo Jin Kim(김수진)

Department of Geological Sciences, Seoul National University, Seoul 151-742, Korea  
(서울대학교 지질학과)

**ABSTRACT:** The Sancheong kaolin was fractionated into 9 size fractions by wet sieving, sedimentation, and centrifugation. The systematic X-ray diffraction combined with electron microscopy shows that the clay mineral composition of each size fraction is related to the original fabric of kaolin.

Minerals such as halloysite (10Å), kaolinite, illite, and goethite which were formed by precipitation from slolution are generally concentrated in the finer fractions, whereas vermiculite which was formed by pseudomorphic transformation from other primary minerals are concentrated in the coarser fractions. Kaolinites of various types which were formed by precipitation or transformation show a wide size range but they are generally concentrated in the coarser fractions. Halloysite or halloysite-kaolinite clusters in coarse fractions are the fragmentation products of the walls of original boxwork kaolin which escaped the complete dispersion even through the grinding, ultrasonic agitation, and chemical treatment.

Separation of fully hydrated halloysite and kaolinite was possible by systematic wet size fractionation. The coarse-grained minerals such as vermiculite and kaolinite are usually removed during the preparation of clay fraction smaller than  $2\mu\text{m}$ , whereas the fine-grained minerals such as illite and goethite are overlooked in X-ray diffraction of the bulk samples because of their minor contents. The systematic wet size fractionation is needed for understanding of the exact mineralogy of kaolin of weathering origin.

**요약 :** 습식체질법, 퇴적법 및 원심분리법을 이용하여 얻어진 산청고령토의 9개 입도분리시료에 대하여 체계적인 X-선 회절 및 주사전자현미분석을 시행한 결과, 각 입도분의 점토광물 조성은 고령토의 원조성과 관련이 있음을 알 수 있었다.

침전작용에 의하여 생성된 10-Å형 할로이사이트, 일라이트 및 침철석은 미세입도분에 농집되고 모광물의 가상으로 생성된 버미큘라이트는 굵은 입도분에 농집된다. 침전작용 및 가상으로 생성된 다양한 유형의 캐올리나이트는 넓은 입도 분포를 보이지만 일반적으로 굵은 입도분에 농집된다. 굵은 입도분의 할로이사이트는 고령토 원래의 망상구조의 파편들인 할로이사이트 또는 할로이사이트와 캐올리나이트의 덩어리들로 존재하며 분쇄, 초음파처리 및 화학처리에 의해 분산되지 않은 것들이다.

체계적인 습식입도분리 실험에 의하여 10-Å형 할로이사이트와 캐올리나이트의 구분도 가능하였다. 버미큘라이트와 캐올리나이트 등의 굵은 광물은  $2\mu\text{m}$  이하의 점토입도분에서는 검출되지 않는 반면 일라이트 및 침철석은 그 양이 적은 경우 원시료만의 X-선 회절분석에서는 검출되지 않는다. 따라서 고령토의 광물조성을 이해하기 위해서는 체계적인 습식입도분리 실험이 필수적이다.

## INTRODUCTION

Residual kaolin formed by weathering commonly contains kaolinite and halloysite

with other minor minerals derived from various precursor minerals. Their sizes are usually not uniform, but variable depending on the environment and the process of formation.

Lombardi *et al.* (1987) reported the compositional and structural variations in both Georgia and Sasso kaolins which are interpreted as due to their different environments of formation. Clay is commonly studied on 2  $\mu\text{m}$  size fraction (Grim, 1968). But such a scheme usually employed in the clay study might result in excluding the coarse minerals larger than 2 $\mu\text{m}$  from the study material.

The Sancheong kaolin has been formed by weathering of anorthosite. It consists chiefly of halloysite and kaolinite with other minor minerals (Jeong, 1987; Kim *et al.*, 1989; Jeong, 1992). Systematic X-ray diffraction and electron microscopic studies of the size fractions of the kaolin show that each mineral in kaolin has a characteristic size range. Present work shows that study restricted to the fine clay fraction only leads to the misunderstanding of the exact mineralogy of kaolin.

## SAMPLES AND METHODS

Two kinds of kaolin samples were selected for size fractionation. One is the white kaolin which contains small amounts of plagioclase, amphibole, and vermiculite. Amphibole and vermiculite occur as green or yellowish brown spots or bands in white kaolin. The other is the highly weathered reddish brown kaolin which contains relatively high amounts of iron oxides.

300g of kaolin sample was blended with distilled water in a 2-liter porcelain mortar and disaggregated by slight grinding. The suspension was further treated with ultrasonic agitation for 5 minutes after a few drops of NaOH solution were added to facilitate dispersion. The suspension was treated for size fractionation applying wet sieving, sedimentation, and centrifugation. The size fraction larger than 74 $\mu\text{m}$  was separated by the wet sieving method repeating three times. The sieved suspension was subsequently transferred to a 2-liter settling cylinder (50cm  $\times$  8cm) and fractionated using sedimentation method to the size fractions; 74–20, 20–10, 10–5, 5–2 $\mu\text{m}$ . Particle diameter was calculated from the settling veloc-

ity using the Stoke's law. The suspension 5cm above the sediment was decanted with a water vacuum pump and transferred to another settling cylinder to obtain finer size fractions by the same method. The sediments per each step were resuspended and repeatedly settled three times. The settled sediments were prepared to wet cake using a filter flask equipped with a water vacuum pump.

The 2–1, 1–0.5, and 0.5–0.1  $\mu\text{m}$  size fractions were prepared by the centrifugation method because size fractionation of so extremely fine size fractions by sedimentation took too long time. The centrifugation time for the particular size fraction was calculated by the equation of Svedberg and Nichols (1923). The settled sediments on the bottom of the tube were resuspended by ultrasonic agitation and repeatedly centrifuged three times further. The size fraction smaller than 0.1 $\mu\text{m}$  was difficult to separate even by the centrifugation, so that it was separated by centrifugation after the complete flocculation with NaCl. All the separated size fractions were preserved in the wet cake state to prevent the dehydration of halloysite throughout the process. The calculation of settling and centrifugation time for separating specific size fraction assumes that the particle has a smooth spherical shape. Therefore, the sizes mentioned below are the equivalent spherical diameter.

Systematic investigation using X-ray diffraction (XRD) and scanning electron microscopy (SEM) was carried out for the size fractions of kaolin. XRD patterns were recorded from wet cake packed in the cavity of aluminum holder using Rigaku RAD3-C automatic X-ray diffractometer with Ni-filtered CuK $\alpha$  X-ray radiation generated at 35kV/20mA. Formamide intercalation was carried out to distinguish halloysite from kaolinite according to the procedure of Churchman *et al.*, (1984). For intercalation, the reagent grade formamide solution was sprayed on the air-dried size fractions smeared on the glass slides.

Dry cake was glued to copper stub using colloidal graphite adhesive and coated with

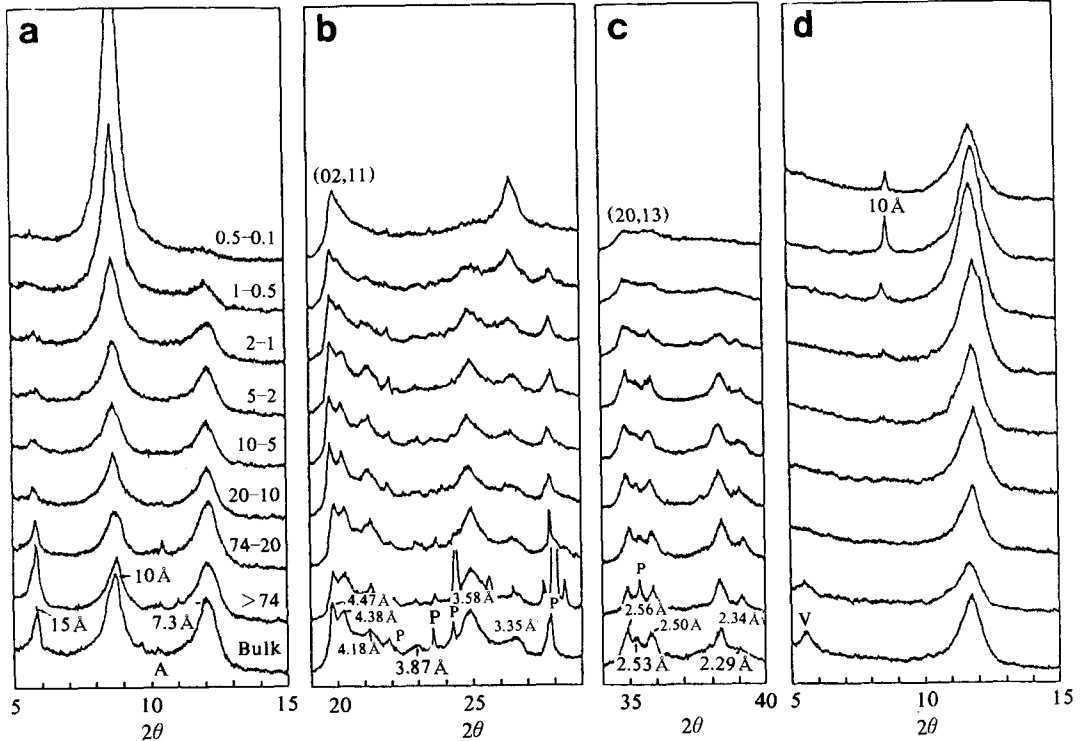


**Fig. 1.** X-ray diffraction patterns of bulk and 8 size fractions of white kaolin. (a)  $5^{\circ}\sim 15^{\circ}$  (random mounts), (b)  $19^{\circ}\sim 29^{\circ}$  (random mounts), (c)  $34^{\circ}\sim 40^{\circ}$  (random mounts), (d)  $5^{\circ}\sim 15^{\circ}$  (dried at  $60^{\circ}\text{C}$ , oriented mounts). Ni-filtered  $\text{CuK}\alpha$  radiation. Sizes indicated in (a) are in  $\mu\text{m}$  unit. A: amphibole, P: plagioclase, V: vermiculite.

gold for SEM by secondary electron image mode. JEOL 733 Superprobe instrument equipped with Link energy dispersive spectrometer (EDS) was used for qualitative element analysis as well as SEM observation. SEM was also carried out for the undisturbed kaolin sample to observe original fabrics of kaolin by back-scattered electron image mode. Clay suspension was loaded on the carbon-coated collodion film for transmission electron microscopy (TEM). JEOL JEM 200CX instrument was used at 160kV.

The size fractionation was so tedious that only six kaolin samples were selected for the treatment. The results of two of them are demonstrated in this paper. The others show similar results. Therefore, the data given below reflect the general characteristics of size distribution of each mineral in kaolin.

## RESULTS

### White Kaolin

Sequential XRD analyses of size fractions of kaolin in the range of  $5^{\circ}\sim 15^{\circ}(2\theta)$  (Fig. 1a) show that the peak intensities of three basal reflections of 15, 10, and 7.3 Å vary systematically with particle size. High quality XRD pattern for the fraction smaller than  $0.1\mu\text{m}$  could not be obtained because of its low recovery.

15-Å reflection is due to vermiculite as evidenced by both ethylene glycolation and heat treatment. The intensity of 15-Å reflection of vermiculite is maximum in the fraction larger than  $74\mu\text{m}$  and gradually decreases toward finer fractions.

The intensity of 10-Å reflection gradually increases toward finer fractions. The XRD

pattern of 0.5–0.1  $\mu\text{m}$  fraction shows only 10-Å reflections with trace of 7.3-Å reflection. This finest fraction consists mostly of tubular halloysite as confirmed by the TEM observation (Jeong, 1992). The sharp and symmetrical peak shape of 10-Å reflection in the XRD pattern of the 0.5–0.1  $\mu\text{m}$  implies that halloysite of the Sancheong area is in the hydrated state under natural weathering environment.

The intensity of 7.3-Å reflection is maximum in 74–20  $\mu\text{m}$  fraction and, then, gradually decreases toward finer fractions. The peak splittings in the regions of 19°–24° (Fig. 1b) and 34°–40° ( $2\theta$ ) (Fig. 1c) are apparent in the 74–20  $\mu\text{m}$  fraction, but with decreasing size, they become gradually weak and finally disappear in the 0.5–0.1  $\mu\text{m}$  fraction. 02, 11 and 20, 13 reflection regions tailing toward high angle appear in the 0.5–0.1  $\mu\text{m}$  fraction. Such phenomena are consistent with the increasing intensity of 10-Å reflection and the decreasing intensity of 7.3-Å reflection toward fine fractions. The systematic change of XRD patterns of 8 size fractions strongly indicates that the 10-Å and 7.3-Å reflections in the XRD patterns of kaolin are due to hydrated halloysite (10Å) and kaolinite, respectively.

In order to know whether or not illite is present in white kaolin, sequential XRD analyses were carried out for the size-fractionated kaolin samples which were dried at 60°C for 5 hours (Fig. 1d) because the strong 10-Å reflection of halloysite in kaolin shielded the 10-Å reflection of illite. The dehydration temperature was selected from the experimental result that vermiculite dehydrated above 150 °C, and halloysite (10Å) easily dehydrated to halloysite (7Å) by heating at 60°C. Fig. 1d shows that the less intense 10-Å reflection still remains after dehydration. This fact suggests that illite is present above 5  $\mu\text{m}$  and increases toward finer fractions.

Detrital grains of plagioclase and amphibole are concentrated in the coarse fractions above 20  $\mu\text{m}$  but small plagioclase peak at 3.18 Å still persists down to 1–0.5  $\mu\text{m}$  fraction.

Mineral compositions determined by XRD analysis of both the various size frac-

**Table 1.** Semiquantitative mineral composition of various size fractions of Sancheong Kaolin.

Size ( $\mu\text{m}$ )	White kaolin						Reddish brown kaolin	
	V	H	K	I	P	A	H	K
Bulk	5.9	24.6	67.1	0.0	2.2	0.2	24.7	75.3
>74	9.7	14.5	64.5	0.0	10.9	0.4	7.0	93.0
74–20	4.3	14.3	77.7	0.0	2.9	0.8	11.9	88.1
20–10	2.1	22.6	72.9	0.0	2.4	0.0	19.8	80.2
10–5	2.4	28.6	66.4	0.0	2.4	0.0	32.3	67.7
5–2	1.4	30.1	65.1	1.2	2.2	0.0	36.6	63.4
2–1	1.6	43.4	51.3	1.9	1.8	0.0	41.2	58.8
1–0.5	0.0	68.3	26.0	4.7	1.0	0.0	54.4	45.6
0.5–0.1	0.0	92.4	4.6	3.0	0.0	0.0	89.0	11.0
<0.1							100.0	0.0

V: vermiculite, H: halloysite(10Å), K: kaolinite, I: illite, P: plagioclase, A: amphibole.

tions of white and reddish brown kaolins are given in Table 1. In the white kaolin, vermiculite, kaolinite, plagioclase, and amphibole are concentrated in coarse fractions, whereas halloysite (10Å) and illite in fine fractions. It is notable that quantitative analyses of bulk sample do not detect illite which is contained about 5% in 1–0.5  $\mu\text{m}$  fraction, whereas quantitative analyses of the fraction smaller than 1  $\mu\text{m}$  do not detect vermiculite which is contained about 6% in bulk sample.

SEM photograph of 74–20  $\mu\text{m}$  fraction (Fig. 2a) of white kaolin shows various stacks, irregular aggregates, and corroded plagioclase. EDS analysis shows that the thin micaceous stacks consist of vermiculite, and the quite long stacks with more or less euhedral form, clean edges, and longitudinal grooves of kaolinite. The aggregates are virtually compactly agglomerated halloysite or halloysite-kaolinite clusters where small vermiform kaolinite stacks are enclosed by cryptocrystalline halloysites. Plagioclase has clean surface with etch pits. Both halloysite and kaolinite are not in direct contact with plagioclase.

SEM photograph of 5–2  $\mu\text{m}$  fraction (Fig. 2b) shows kaolinite stacks and fuzzy halloysite clusters. The content of kaolinite stacks of this fraction is low as compared with 74–20  $\mu\text{m}$

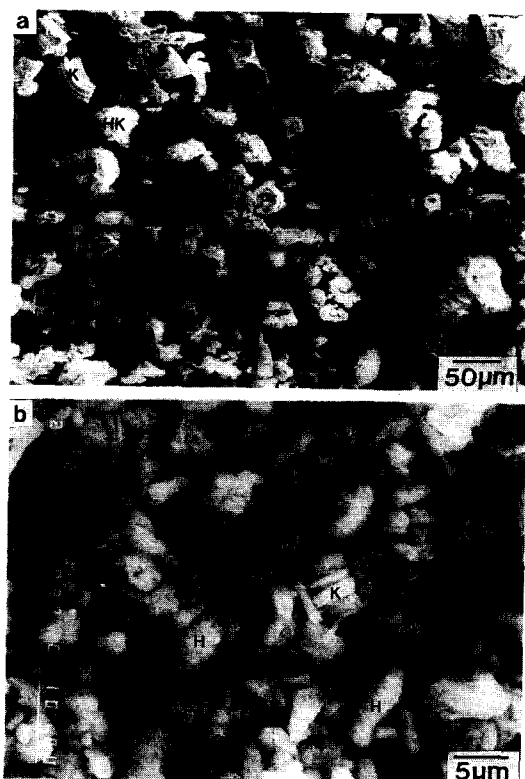


**Fig. 2.** Electron micrographs of two different size fractions of white kaolin. (a) SEM photograph of 74–20  $\mu\text{m}$  fraction of white kaolin showing kaolinite stacks (K), vermiculite stacks (V), clusters of halloysite and kaolinite (HK), and corroded plagioclase (P), (b) SEM photograph of 5–2  $\mu\text{m}$  fraction showing kaolinite stacks (K) and fuzzy halloysite clusters (H).

fraction, whereas that of halloysite clusters is high. Vermiculite flake or plagioclase particle is not found in the photograph although the very weak peaks of vermiculite and plagioclase are detected in the XRD analysis.

### Reddish Brown Kaolin

Sequential XRD analysis in the range of  $5^\circ$ – $15^\circ$  ( $2\theta$ ) (Fig. 3a) show only two reflections at 10 and 7.3 Å. Vermiculite peak at 15 Å is absent in the reddish brown kaolin. The intensity of 10-Å reflection gradually increases toward the finer fractions. Only one sharp and symmetrical 10-Å reflection is found in the

finest fraction smaller than 0.1  $\mu\text{m}$ . This fact indicates that halloysite in the reddish brown kaolin is also in the fully hydrated state as in the white kaolin. The intensity of 7.3-Å reflection is maximum in the fraction larger than 74  $\mu\text{m}$ , and then, decreases gradually toward finer fractions.

Systematic changes of the XRD patterns of both the white and reddish brown kaolins indicate that the 7.3-Å reflection is not due to halloysite (7 Å) but due to kaolinite. The hydrated state of halloysite and nature of 7.3-Å in kaolin could be confirmed by other auxiliary method. Churchman *et al.* (1984) recommended the formamide intercalation method for critically differentiating halloysite from kaolinite. They showed that if the halloysite was not dehydrated above  $110^\circ\text{C}$  before intercalation, halloysite-formamide complex is formed both rapidly and completely within 1 hour without regard to the hydration state, whereas no significant kaolinite-formamide complex is formed until at least 4 hr without regard to the crystallinity of kaolinite. Formamide intercalation test was carried out for the air-dried size fractions of 74–20  $\mu\text{m}$  and 5–2  $\mu\text{m}$ . The results are given in Fig. 4. Major changes of XRD patterns occurred rapidly within 30 min, and further notable change was not observed after long time duration up to 4 hr. 10.4-Å and 7.3-Å reflections are due to halloysite-formamide complex and unreacted kaolinite based on the criterion of Churchman *et al.* (1984). The relative intensities of 10.4-Å and 7.3-Å reflections after intercalation are highly similar to those of wet size fractions (Fig. 4). This fact confirms that the 10-Å and 7.3-Å reflections are due to the hydrated halloysite (10 Å) and kaolinite, respectively. The broad half width and low height of basal reflections of kaolinite make it very difficult to distinguish it from the dehydrated halloysite (7 Å).

The peak splittings in the range of  $19^\circ$ – $24^\circ$  ( $2\theta$ ) (Fig. 3b) and  $34^\circ$ – $40^\circ$  ( $2\theta$ ) (Fig. 3c) become weaker toward the finer fractions. It is notable that the reddish brown kaolin contains microcrystalline goethite. The strongest 4.18-Å re-

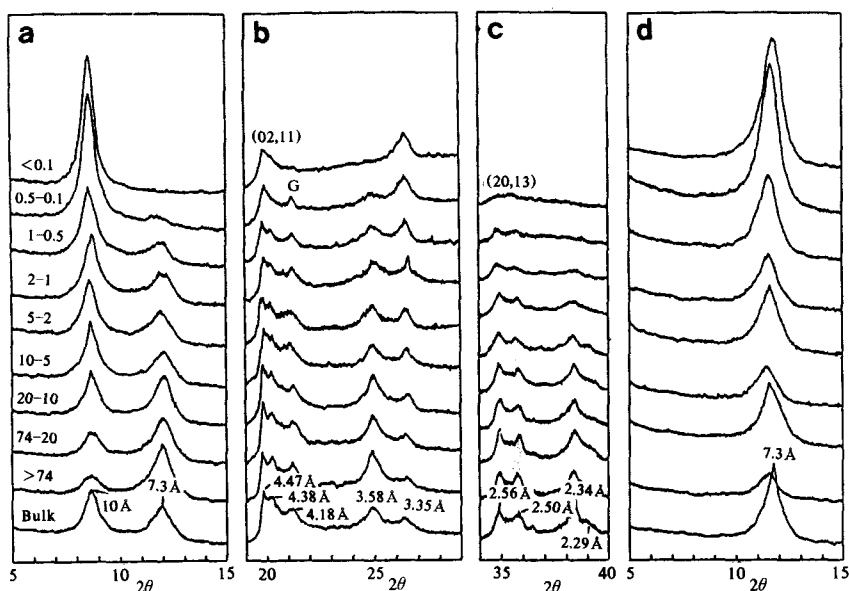


**Fig. 3.** X-ray diffraction patterns of bulk and 9 size fractions of reddish brown kaolin. (a)  $5^{\circ}$ – $15^{\circ}$  (random mounts), (b)  $19^{\circ}$ – $29^{\circ}$  (random mounts), (c)  $34^{\circ}$ – $40^{\circ}$  (random mounts), (d)  $5^{\circ}$ – $15^{\circ}$  (dried at  $60^{\circ}\text{C}$ , oriented mounts). Ni-filtered  $\text{CuK}\alpha$  radiation. Sizes indicated in (a) are in  $\mu\text{m}$  unit. G: goethite.

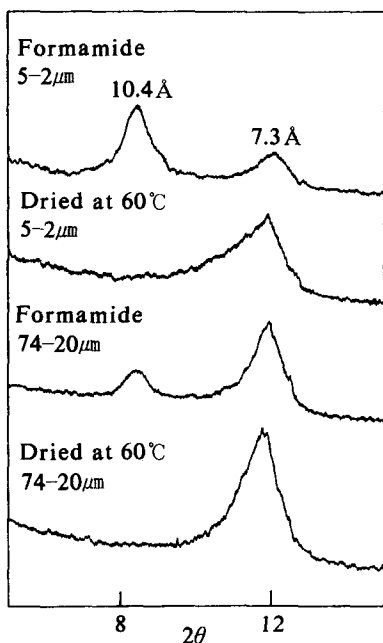


**Fig. 4.** X-ray diffraction patterns of the size fractions dried at  $60^{\circ}\text{C}$  and their formamide intercalates.  $\text{CuK}\alpha$  radiation. Compare the XRD patterns of formamide intercalates and those of corresponding size fractions shown in Fig. 3.

Reflection of goethite is superimposed on the 111 reflection of kaolinite, so that goethite escapes from detection in the coarse fraction, but XRD patterns of fine fractions below  $2\mu\text{m}$  show 4.18-Å reflection of goethite on the 02, 11 reflection region of halloysite (10Å). Goethite persists down to 0.5–0.1 $\mu\text{m}$  fraction.

XRD patterns of size-fractionated samples dried at  $60^{\circ}\text{C}$  for 5 hours (Fig. 3d) show no detectable 10-Å peak. This fact implies that illite is absent in this highly weathered kaolin. Plagioclase and amphibole are not detected in all the fractions of the reddish brown kaolin.

Mineral compositions of the reddish brown kaolin (Table 1) clearly show that halloysite (10Å) and kaolinite have the different size distributions. Fraction larger than 74  $\mu\text{m}$  consists mostly of kaolinite, whereas fraction smaller than 0.1 $\mu\text{m}$  consists entirely of halloysite (10Å).

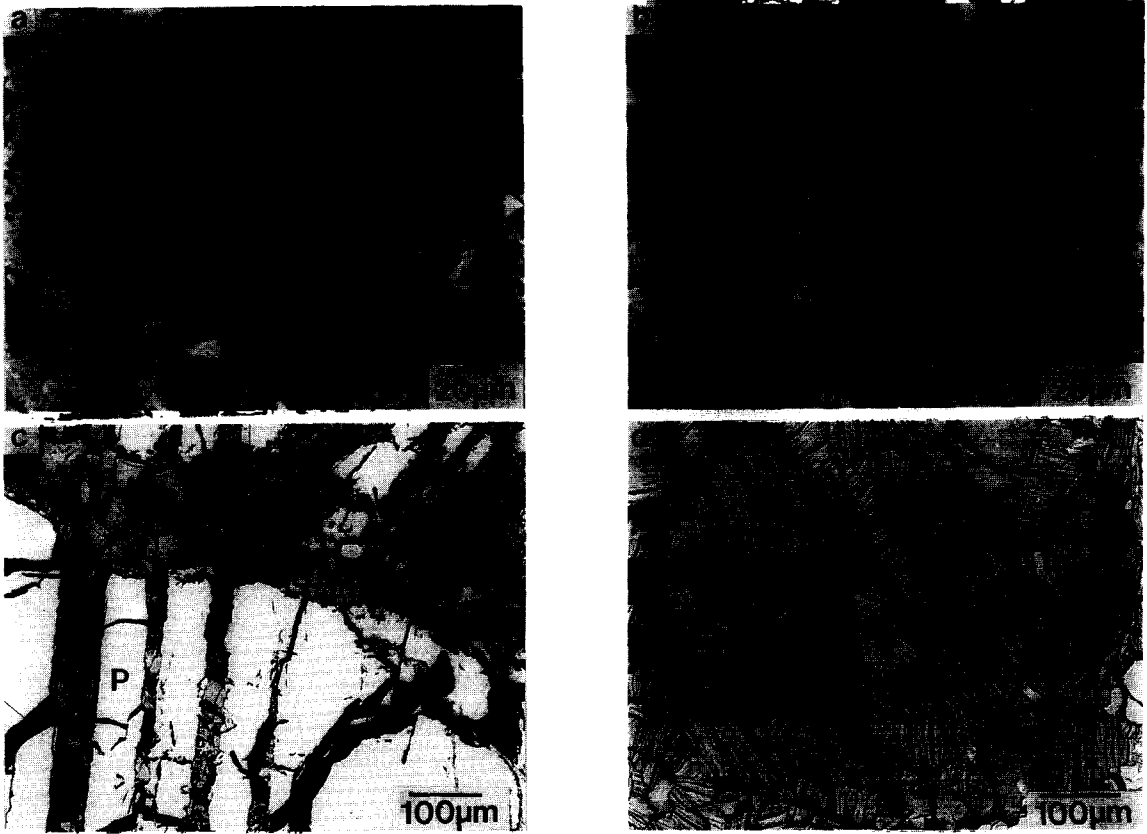


**Fig. 5.** Back-scattered electron micrographs showing the original fabrics of kaolin. (a) Boxworks consisting of compactly agglomerated halloysite walls and large voids, (b) kaolinite stacks (K) enclosed in the halloysite aggregates (H), (c) heterogeneous size distribution of kaolinite stack: large kaolinite stacks derived from vermiculite (K2) and aggregates of small vermiform kaolinite stacks (K1) which were precipitated from solutions, (d) large vermiculite stacks derived from chloritized biotite. P: plagioclase. Black is void. Scale bar = 50 $\mu$ m.

## DISCUSSION

### White Kaolin

Systematic mineralogical analyses (Table 1) of 8 size fractions show that each constituent mineral has a characteristic size range. In the white kaolin, vermiculite, kaolinite, amphibole, and plagioclase tend to concentrate in the coarse fractions, whereas halloysite (10 Å) and illite tend to concentrate in the fine fractions.

Halloysite (10Å) is the only kaolin mineral in the 0.5–0.1 $\mu$ m fraction, but it is present in all the fractions up to 74 $\mu$ m. Although halloy-

site is also present in the coarse fractions, it is not due to its large size, but to the compactly agglomerated halloysite or halloysite-kaolinite clusters as shown in Figs. 3a and 3b. Therefore, the actual size of halloysite particle is smaller than 0.1 $\mu$ m with various length as shown in TEM photograph (Jeong and Kim, 1991; Jeong, 1992). The halloysite clusters are not the flocculation product produced during the size fractionation process, but inherited from the original fabric of kaolin. A study on the microtexture of original kaolins in thin section shows that kaolin in this area usually has a boxwork structure consisting of the numerous thick or thin walls of compactly ag-

lomerated halloysite in a porous cellular pattern as shown in Fig. 5a (Jeong and Kim, 1992a). Small vermiform kaolinite stacks are often enclosed in the halloysite walls (Fig. 5b). Therefore, the halloysite or halloysite-kaolinite clusters in the coarse size fractions are the crushed fragments of those walls which have persisted during the sample preparation process including slight grinding, intensive ultrasonic agitation, and addition of deflocculating agents for size fractionation.

Kaolinite is found in all the size fractions above  $0.5\mu\text{m}$ , but most abundant in the most coarse fraction. Large kaolinite stacks thicker than  $50\mu\text{m}$  are easily observed in the  $74\text{--}20\mu\text{m}$  fraction. The presence of kaolinite over the wide size range might suggest their various sources. Back-scattered electron image for the thin section of undisturbed original kaolin shows various forms of kaolinite stacks of various sizes (Fig. 5c). Jeong (1992) and Jeong and Kim (1992b) have classified the kaolinite stacks in Sancheong kaolin into four different types on the basis of morphology: the vermiform kaolinite which is usually smaller than  $5\mu\text{m}$  in size (type 1) (K1 in Fig. 5c), the columnar kaolinites as thick as  $20\mu\text{m}$  bridging the fissures (type 2), the loosely-stacked kaolinite which is either (Fe, Mg)-rich and as thick as  $50\mu\text{m}$  (type 3) (K2 in Fig. 5c) or K-rich and smaller than  $5\mu\text{m}$  in size (type 4). They interpreted that the kaolinites of types 1 and 2 have been formed by precipitation from solution. The kaolinite of type 3 is the pseudomorphic transformation product of medium-grained vermiculite which was transformed from biotite or chloritized biotite. The kaolinite of type 4 contains minute illite flakes as relics of weathering. These different modes of formation of kaolinite are reflected in their wide size distribution.

Vermiculite occurs as pseudomorphs after chlorite, biotite, and chloritized biotite (Fig. 5d), so that it is concentrated in the coarser fractions. It contains some kaolinite because it is also easily weathered to kaolinite.

Occurrence of microcrystalline illite below  $5\mu\text{m}$  suggests the possibility that it pre-

cipitated from solution. A study on the texture of slightly weathered anorthosite shows that small dioctahedral illite books less than  $5\mu\text{m}$  in thickness are distributed around vermiculite pseudomorphs after biotite (Jeong, 1992). They are interpreted to have been formed by precipitation from high  $a\text{K}^+/a\text{H}^+$  solution near the degrading biotite which released abundant  $\text{K}^+$ . Part of illite in kaolin is believed to have been derived from anorthosite. It is often found under the microscope that microcrystalline illite fills microfractures or grain boundaries in fresh anorthosite (Jeong, 1992).

### Reddish Brown Kaolin

The reddish brown kaolin overlying the white kaolin is more weathered product of the latter. It consists of halloysite ( $10\text{\AA}$ ), kaolinite, and goethite. A study on the 9 size fractions of the reddish brown kaolin shows that plagioclase and amphibole are absent in all the size fractions implying that the precursor minerals in anorthosite have been completely dissolved under the highly leaching condition.

Halloysite ( $10\text{\AA}$ ) and kaolinite show size distributions similar to those of white kaolin. Kaolinite is of structurally disordered type. The Hinckley indices of kaolinite in the reddish brown kaolin is 0.5 in average. Vermiculite and illite were not detected in all the fractions. A study of thin section using electron microprobe analysis and TEM (not illustrated here) shows that both minerals have been altered to kaolin minerals at the late stage of weathering (Jeong, 1992). Vermiculite has completely transformed to large kaolinite stack, whereas illite transformed to halloysite spheres or tubes. Iron which was released during the transformation of vermiculite to kaolinite and the dissolution of amphibole has been precipitated to microcrystalline goethite.

### Size Fractionation in Kaolin Study

It has long been regarded by many workers (Kim and Kim, 1964; Sang *et al.*, 1972; Lee



*et al.*, 1977; Sang, 1980; Kim *et al.*, 1986) that the 10-Å and 7-Å reflections in the XRD pattern of the kaolin from Sancheong are due to halloysite (10Å) and halloysite (7Å), respectively, but the present work shows that halloysite occurs as fully hydrated 10-Å type in natural state and that 7-Å reflection is due to kaolinite. The difficulty of distinction between halloysite (10Å) and kaolinite could be overcome by the systematic wet size fractionation combined with formamide intercalation. It is significant to mention that kaolinite is more abundant in the Sancheong kaolin than ever expected.

The present study shows that in the research on the halloysitic clay originated from the weathering of crystalline rocks, the systematic wet size fractionation is indispensable for understanding of the exact mineralogy of kaolin and their size distribution. Size fractionation with more narrow interval may give more better information. The present study also shows that the study on the clay fraction smaller than 2 $\mu$ m which is usually employed in clay study leads to misunderstanding of the exact mineralogy of the raw clay materials. The minerals larger than 2 $\mu$ m such as vermiculite and kaolinite are removed during the preparation of study material by the commonly employed method, whereas the bulk sample study may fail to detect the minor fine-grained minerals such as illite and goethite. Therefore, the systematic wet size fractionation for the raw kaolin is needed for understanding of its exact mineralogy.

In addition, the systematic size fractionation also gives an important information for the beneficiation of kaolin. Present study shows that compactly agglomerated halloysite or halloysite-kaolinite clusters which were originated from boxwork kaolin are concentrated in coarse fractions larger than 2 $\mu$ m. Pure mineral samples for detailed mineralogical study can be prepared by the repeated size fractionation. For example, the pure halloysite (10Å) sample can be obtained by separation of size fraction smaller than 0.1 $\mu$ m, whereas a large amount of vermiculite flake

can be obtained by the magnetic separation and hand-picking from the size fractions larger than 20 $\mu$ m.

## CONCLUSIONS

Each mineral in the Sancheong kaolin has a characteristic size range depending on its formation process. Minerals such as halloysite (10Å), kaolinite, illite, and goethite which were formed by precipitation from solution are generally concentrated in the finer fractions, whereas minerals such as vermiculite and kaolinite which were formed by pseudomorphic transformation from coarse precursor minerals are concentrated in the coarser fractions. Original fabrics of kaolin influences the mineral composition of size fractions without regard to the real size of constituent minerals. The halloysite or halloysite-kaolinite clusters in coarse fractions are the fragmentation products of original boxworks. Therefore, the mineral composition of clay minerals in each size fraction is related to the fabric of kaolin which is in turn related to the formation mechanism of clay minerals.

The separation of fully hydrated halloysite and kaolinite is also possible by the systematic wet size fractionation. The coarse-grained minerals such as vermiculite and kaolinite are usually removed during the preparation of clay fraction smaller than 2 $\mu$ m by the commonly employed method, whereas the fine-grained minerals such as illite and goethite are overlooked in X-ray diffraction of the bulk samples because of their minor contents. The systematic wet size fractionation is needed for understanding of the exact mineralogy of kaolin.

## REFERENCES

- Churchman, G. J., Whitton, J. S., Claridge, G. G. C., and Theng, B. K. G. (1984) Intercalation method using formamide for differentiating halloysite from kaolinite. *Clays Clay Miner.* 32, 241-248.
- Grim, R. E. (1968) *Clay Mineralogy*, 2nd edi-

- tion, McGraw-Hill, New York, 1-2.
- Jeong, G. Y. (1987) Mineralogy and genesis of kaolin from Sancheong area. MS thesis, Seoul National University, Korea.
- Jeong, G. Y. (1992) Mineralogy and Genesis of Kaolin in the Sancheong District, Korea. Ph. D. Thesis, Seoul National University, 325p.
- Jeong, G. Y. and Kim S. J. (1992a) Boxwork structure of halloysite-rich kaolin formed by weathering of anorthosite in Sancheong area, Korea. Abstracts, 29th Inter. Geol. Cong., Kyoto, 711.
- Jeong, G. Y. and Kim, S. J. (1992b) Kaolinites in the Sancheong kaolin, Korea: their textures, chemistry, and origin. Clay Minerals, Their Natural Resources and Uses, Proc. Workshop WB-1, 29th Inter. Geol. Cong., Kyoto, 129-135.
- Jeong, J. G. (1980) Petrogenesis of anorthosite and related rocks in Hadong-Sancheong district, Korea. PhD thesis, Seoul National University, Korea.
- Keller, W. D. (1970) Environmental aspects of clay minerals. *J. Sed. Pet.* 40, 788-813.
- Kim, S. J., Jeong, G. Y., Lee, S. J., and Kwon, S. K. (1989) Mineralogy of kaolin from Hadong-Sancheong area. *J. Miner. Soc. Korea* 2, 11-17.
- Kim, J. H. and Kim, D. H. (1964) Investigation report of the Sancheong-Gun, Kyeongsang-Namdo, Korea. in *Geology and Ore Deposits*, 7, Geol. Surv. Korea, 67-96. (in Korean)
- Kim, M. Y., Lee, D. J., Shin, H. J., and Lee, S. R. (1986) Studies on comprehensive utilization of domestic kaolin: Mineralogy of kaolin ores. Korea Inst. of Ener. Resour. (in Korean).
- Lombardi, G., Russell, J. D., and Keller, W. D. (1987) Compositional and structural variations in the size fractions of sedimentary and a hydrothermal kaolin. *Clays Clay Miner.* 35, 321-335.
- Lee, S. M., Kim, S. J., and Jeong, J. G. (1977) Mineralogy and genesis of the clay deposits in the Hadong-Sancheong area. *J. Geol. Soc. Korea* 13, 1-14. (in Korean)
- Sang, K. N. (1980) Mineralogy and genesis of halloysite deposits at the Hadong-Sancheong area. PhD thesis, Univ. Tokyo.
- Sang, K. N., Kim, D. H., and Cho, H. I. (1972) Geological and mineralogical studies of kaolin and clay deposits in Hadong-Sancheong district. *Geol. Surv. Korea.* (in Korean)
- Svedberg, T and Nichols, J. B. (1923) Determination of size and distribution of size of particle by centrifugal methods. *J. Amer. Chem Soc.* 45, 2910-2917,